# Supporting Information

## FRET-Based Mesoporous Organosilica Nanoplatforms for *In Vitro* and *In Vivo* Anticancer Two-Photon Photodynamic Therapy

Nicolas Bondon [a, b, *], Clément Charlot [a], Lamiaa M. A. Ali [c, d], Alexandre Barras [e], Nicolas Richy [b], Denis Durand [c], Yann Molard [b], Grégory Taupier [b], Erwan Oliviero [a], Magali Gary-Bobo [c], Frédéric Paul [b], Sabine Szunerits [e], Nadir Bettache [c], Jean-Olivier Durand [a], Christophe Nguyen [c], Rabah Boukherroub [e], Olivier Mongin [b, *] and Clarence Charnay [a, *]

[a] ICGM, University of Montpellier, UMR-CNRS 5253, 34293 Montpellier, France

[b] Univ Rennes, CNRS, ISCR (Institut des Sciences Chimiques de Rennes) - UMR 6226, ScanMAT – UAR 2025, F-35000, Rennes, France

[c] IBMM, University of Montpellier, UMR-CNRS 5247, 34293 Montpellier, France

[d] Department of Biochemistry, Medical Research Institute, Alexandria University, Alexandria, 21561, Egypt

[e] Univ. Lille, CNRS, Univ. Polytechnique Hauts-de-France, UMR 8520-IEMN, 59000 Lille, France

*Correspondence: nicolas.bondon@concordia.ca (N.B.); olivier.mongin@univ-rennes1.fr@umontpellier.fr (O.M.); clarence.charnay@umontpellier.fr (C.C.);

Tel.: +33-4-48-79-21-26 (C.C.)

# SUMMARY:

# EXPERIMENTAL SECTION:

## A) Characterization

$^{1}$H NMR spectrum of P-Si was obtained with a Bruker Avance 400 MHz NMR spectrometer (Billerica, MA, USA) equipped with a BBSO probe.

Samples for transmission electron microscopy (TEM) measurements were deposited from suspensions on Cu Formvar/C holey grids and allowed to dry before observation. The main TEM images were acquired using a JEOL 1400 Flash operated at 120 kV. The quantification of the NPs diameters was performed with the ImageJ software with at least 100 counts. The elemental mapping was recorded in STEM mode with an Oxford Instruments XMaxN 100 TLE (100 $mm^2$, windows less) EDX detector connected to a JEOL 2200 FS (FEG) Transmission Electron Microscope operated at 200 kV with a Gatan UltraScan 4000 (4k x 4k) CCD camera. CHNS elemental analyses were performed on a Elementar Vario Micro Cube (Langensenbold, Germany).

Hydrodynamic diameter and zeta potential measurements were recorded on Malvern NanoSeries (Malvern, UK) Zetasizer NanoZS (model ZEN3600) in a DTS1060C Zetacell (for the zeta potential) at 25 °C, with an equilibration time of 60 s and with automatic measurement, and data were treated by Zetasizer software using a Smoluchowski model.

$N_2$ adsorption and desorption were measured at 77 K using a Micromeritics TriStar (Norcross, GA, USA) device (V6.06 A). Prior to the sorption experiment, the samples were dried under vacuum at 80 °C for 8 h. Specific surface areas (SSAs) were obtained *via* the Brunauer-Emmett-Teller method.[1] Pore size distributions were obtained from the desorption branch of the nitrogen isotherm using the Barrett–Joyner–Halenda equation.

Solid-state NMR spectra were acquired on a 300 MHz Varian VNMRS300 spectrometer (Les Ulis, France) equipped with a "wide-bore" magnet at 7.05 T, using a Varian T3 MAS (Magic Angle Spinning) probe with 3.2 mm $ZrO_2$ rotors. $^{13}$C NMR spectra in cross polarization-MAS mode have been acquired with a recycle delay of 3 s and a contact time of 1 ms. A sample of adamantane has been used as a secondary reference (left peak at 38.5 ppm). The samples spun at a spinning speed of 12 kHz, the width of the spectral window was 50 kHz, and the line broadening was 50 Hz.

Electron spin resonance (ESR) measurements were recorded with an Elexsys E500 Bruker EPR spectrometer in Xband of around 9.8 GHz at room temperature by using a sealed capillary. Instrument settings were: modulation amplitude: 1.0 G; microwave power: 20 mW; time constant: 10.24 ms; sweep time: 20.97 s; frequency modulation: 5 kHz; coupling constant: 17.2 G; G-factor: 2.0056. Hyperfine splitting constants were measured directly from spectra.

## B) Methods

### 1) 11-(Aminoundecyl)triethoxysilane (AUTES) titration by fluorescamine primary amine assay and grafting estimation

AUTES ($M_w$ = 333.59 g mol$^{-1}$, d = 0.895) grafting was quantified by fluorescence using fluorescamine, which is known to undergo reaction with primary amines. Briefly, a 3:1 (v:v) solution 1 was prepared by mixing fluorescamine (1 mg mL$^{-1}$ in DMSO) with a buffer borate solution (pH 8.5) prepared from boric acid and basified with a 200 mM NaOH aqueous solution. Then, each AUTES standard or F-P PMO@PEG sample (solution 2, in EtOH) was mixed with solution 1 in a 1:1 (v:v) ratio. The final AUTES standard concentrations were 2.37, 5.92, 11.83 and 23.66 µg mL$^{-1}$, and the final NPs samples' concentration was 500 µg mL$^{-1}$. Finally, the grafting amounts were calculated from the fluorescence intensities ($\lambda_{em.}$, max = 482 nm, $\lambda_{exc.}$ = 390 nm, voltage = 645 V) obtained with a Safas Xenius XM microplate reader (Monaco), using a standard curve with linear correlation. PEG-Si ($M_w$ = 410.62 g mol$^{-1}$) and MAN ($M_w$ = 393.33 g mol$^{-1}$) grafting efficiencies were estimated considering the 25:1 (mol:mol) PEG-Si:AUTES and 1:1 (mol:mol) AUTES:MAN ratio. Equation (1) was employed to determine the necessary amount of MAN to put in reaction to reach full coverage of amine functions (*vs.* grafted NPs):

$$m(MAN) = \frac{[AUTES]\ Mw\ (MAN)}{Mw\ (AUTES)}\ x\ \frac{m\ (F{-}P\ PMO@PEG)}{(1 + [AUTES] + [PEG{-}Si])} \quad (1),$$

where [AUTES] and [PEG-Si] are the mass concentrations *vs.* bare NPs (in µg mg$^{-1}$), and m (F-P PMO@PEG) is the amount of grafted NPs (in mg) introduced for MAN grafting.

**2) Biodegradability simulation studies in the presence of mercaptoethanol**

Briefly, previously vacuum-dried E-4S-F-P PMO NPs (5 mg) were dispersed in an aqueous medium (5 mL) composed of 10 mM PBS and 10 mM mercaptoethanol (equivalent of GSH). The suspension was agitated at slow speed for 7 days, and aliquots were collected at different times for TEM screening.

**3) Cytotoxicity study - MDA-MB-231**

MDA-MB-231 cells were seeded in 96-well plates (Greiner Bio-One, Germany) at a density of 6000 cells *per* well. Twenty-four hours after seeding and growth to an appropriate confluency, cells were treated with different concentrations of ENE-4S-based PMO NPs for 24 h in triplicates to ensure statistical significance. After 3 days of incubation, cell viability was assessed by CellTiter-glo assay (Promega). This viability assay is based on quantification of the ATP present in living cells, a lysis of living cells and the generation of a luminescent signal proportional to the amount of ATP present. The luminescence was measured, and the percentage of cell viability was calculated according to the following equation: ($Lum_{test}/Lum_{control}$ *100).

**4) Cell internalization study – MDA-MB-231**

MDA-MB-231 cells were seeded in glass bottom 8-well tissue culture chambers (World Precision Instrument, Stevenage, UK) at sub-confluence. Twenty-four hours after seeding, cells were treated with 50 µg $mL^{-1}$ of ENE-4S-based PMO NPs for 24 h. Untreated cells were considered as a control. Fifteen minutes before the end of incubation, cells were treated with Hoechst 33342™ (5 µg $mL^{-1}$, Invitrogen) for nuclear staining and with CellMask™ Orange (5 µg $mL^{-1}$, Invitrogen) for membrane staining. Cells were washed three times with culture medium before observation with LSM780 live confocal fluorescence microscope (Carl Zeiss Microscope) equipped with a tunable femtosecond laser chain (Ti-Sapphire Chameleon Ultra II, Coherent with pulse picker, generating 140 fs wide pulses at 80 MHz rate) and excited at 405 nm for nuclei, at 561 nm for cell membranes, and at 780 nm for NPs (TPEF), using for all a high magnification (63×/1.4 OIL DIC Plan-Apo).

**5) Two-photon excitation photodynamic therapy – MDA-MB-231**

MDA-MB-231 cells were seeded into 384-well plates (Corning™ 4581) with 0.17 mm glass bottom at a density of 2000 cells *per* well in 50 µL of culture medium and allowed to grow for 24 h. Then, cells were incubated with or without ENE-4S-based PMO NPs at 50 µg $mL^{-1}$ for 5 or 20 h. Untreated cells were considered as a control. After incubation with NPs, cells were maintained in fresh culture medium, and then submitted (or not) to TPE with the LSM780 NLO microscope (Carl Zeiss Microscope). One third of the well was irradiated at 780 nm by three scans of 1.26 s duration in four different areas of the well with a focused laser at a maximum laser power, not to irradiate overlapping areas. The laser beam was focused with a microscope objective lens (10×) at maximum laser power (3 W input, 900 mW $cm^{-2}$ output before the objective). The scan size does not allow irradiating more areas without overlapping. After 48 h, the phototoxicity was assessed using CellTiter-glo assay. We can establish a percentage of cell viability according to the following equation:

$$\frac{Luminescence\ in\ the\ well}{Luminescence\ in\ the\ control\ well} \times 100,$$

then, the viability was corrected according to the following formula:

(non-irradiated viability – 3 × (non-irradiated viability – irradiated viability)).

Data are mean values standard deviation from three independent experiments.

-

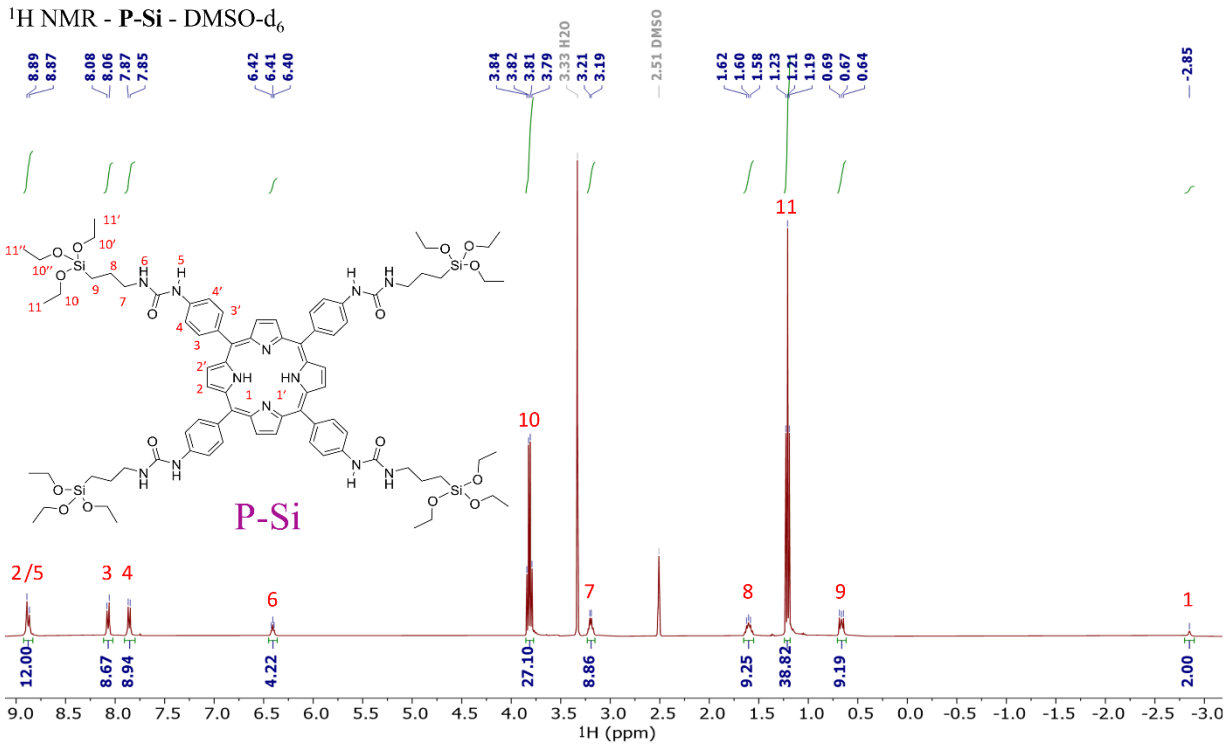


**Figure S1.** $^1$H NMR spectrum of silylated porphyrin (P-Si, in DMSO-$d_6$).

| PMO NPs | Molar % of precursors for the synthesis (premix) | | | | |
|---|---|---|---|---|---|
| | E | ENE | 4S | F-Si | P-Si |
| E-F-P | 95 | | | 0.5 | 4.5 |
| E-4S-F-P | 76 | | 19 | 0.5 | 4.5 |
| ENE-F-P | | 95 | | 0.5 | 4.5 |
| ENE-4S-F-P | | 76 | 19 | 0.5 | 4.5 |

**Table S1.** Synthesis conditions of F-P PMO Nanoparticles (NPs).

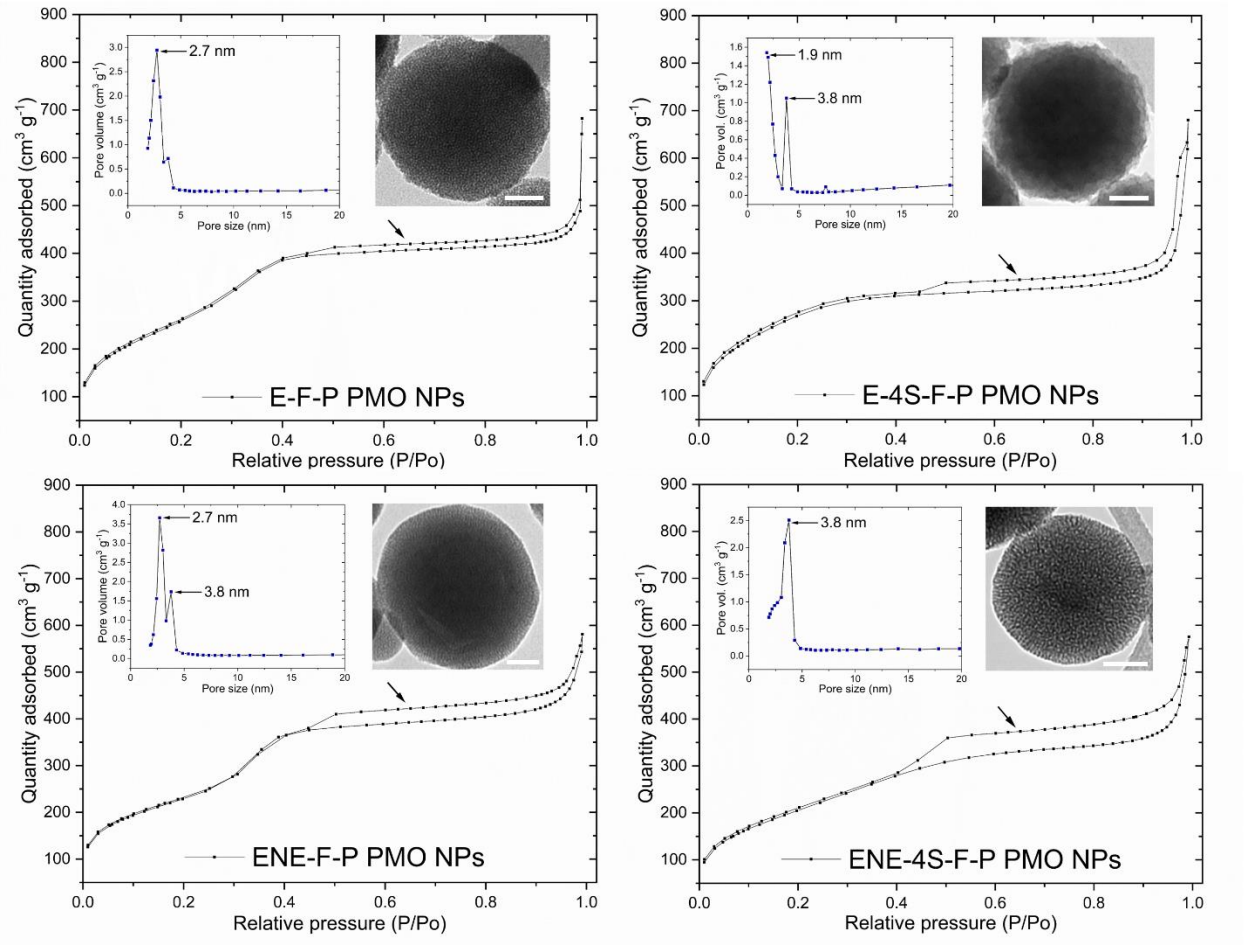


**Figure S2.** $N_2$ sorption type-IV isotherm curves and pore distribution profiles of different pristine F-P PMO NPs. Pore distributions were calculated from the desorption branch of isotherms and using the Barrett–Joyner–Halenda equation. Black arrows indicate a regular hysteresis loop at high relative pressure. Scale bars: 50 nm.

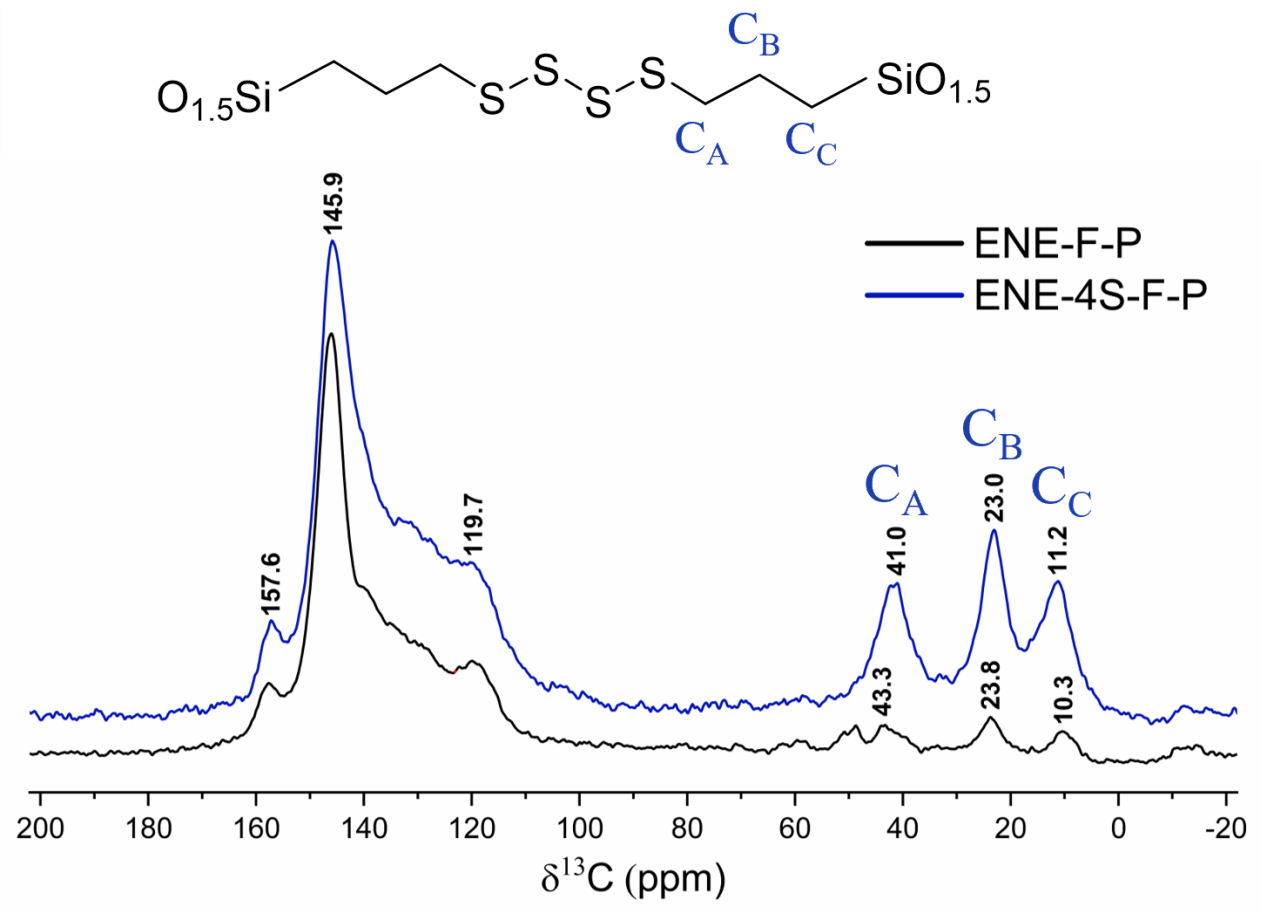


**Figure S3.** $^{13}C$ cross-polarization MAS solid-state NMR spectra. ENE-F-P (black) and ENE-4S-F-P (blue) pristine PMO NPs are represented as well as 4S moieties structure within corresponding PMO framework.

To confirm whether fluorophore F and porphyrin P moieties were integrated in the three-dimensional PMO framework, $^{13}C$ chemical shifts were screened by solid NMR spectroscopy of ENE-F-P and ENE-4S-F-P NPs. The most intense carbon chemical shift observed at 145.9 ppm is attributed to $sp^2$ C=C linkers from ENE precursor.[2,3] Peaks at 150 to 110 ppm are attributed to aromatic carbons and other arylenes from F and P, and the signal at 157.6 ppm is assigned to C=O groups in carbamate and urea groups.[4]

Comparison of alkyl chains between ENE-4S-F-P and ENE-F-P (< 50 ppm) clearly evidence the integration of 4S with peaks from R-S-$C_A$-$C_B$-$C_C$-Si-R′ environment at 41.0, 23.0 and 11.2 ppm, for $C_A$, $C_B$ and $C_C$, respectively. For ENE-F-P, since there is no 4S in the reaction mixture, the signals at 43.3, 23.8 and 10.3 ppm can be attributed to the carbons from F-Si and P-Si moieties between Si atoms, and in the carbamate and urea groups, respectively for F-Si and P-Si.

Altogether, these results indicate the presence of both F, P and 4S within the NPs.

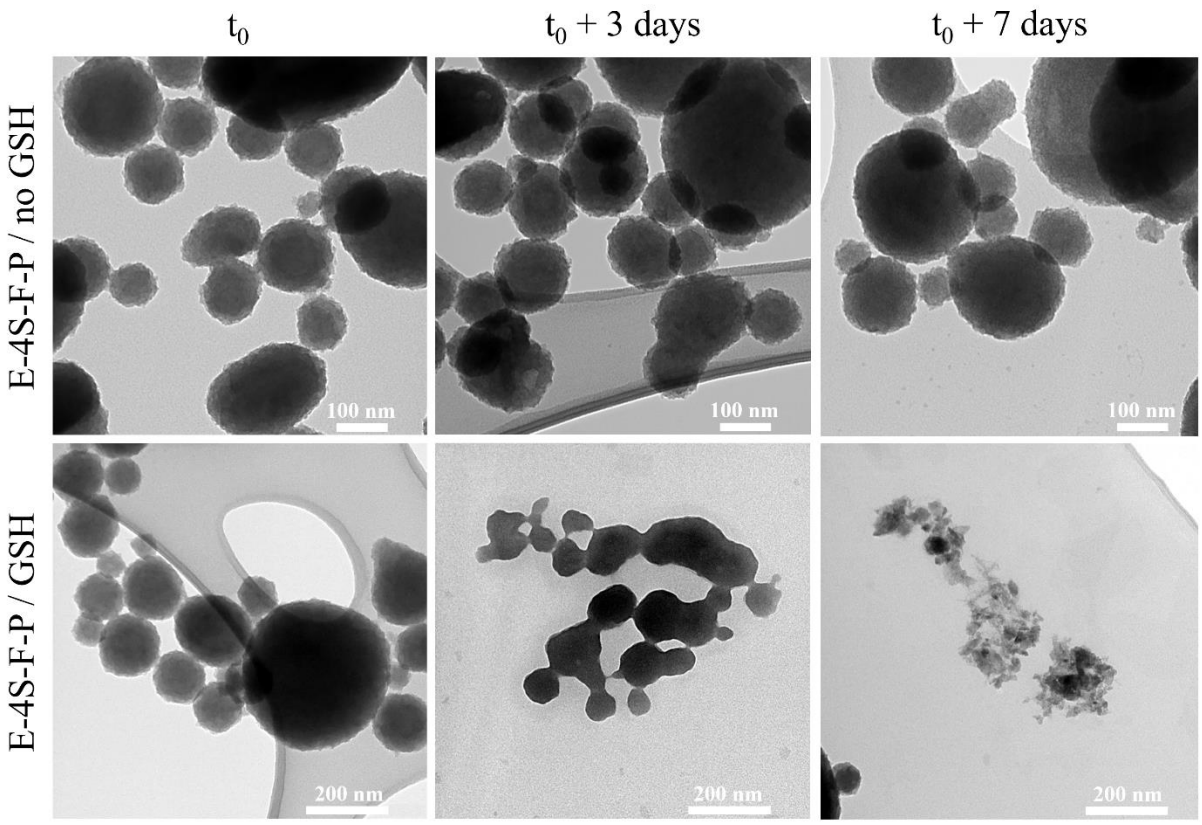


**Figure S4.** Biodegradability studies of 4S-based PMO NPs. TEM images of pristine E-4S-F-P PMO NPs in absence (top) or in presence (down) of simulated GSH-rich biological environment using 10 mM mercaptoethanol. Samples were slightly stirred in PBS (with or without mercaptoethanol) and aliquots were collected at different times before TEM screening.

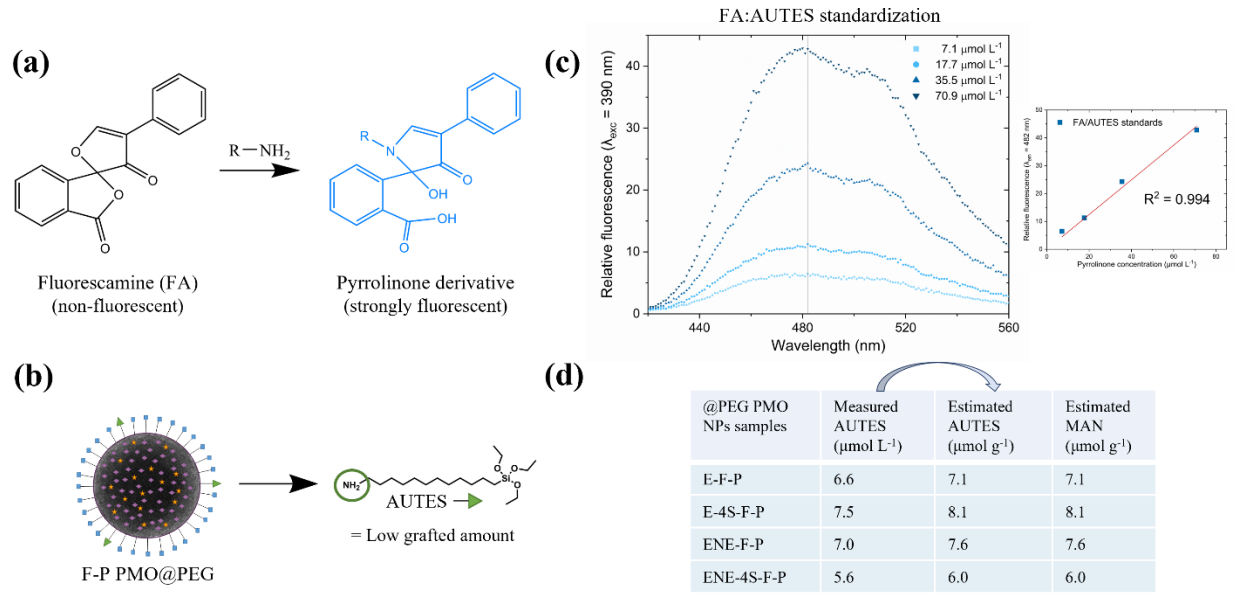


| @PEG PMO NPs samples | Measured AUTES (µmol $L^{-1}$) | Estimated AUTES (µmol $g^{-1}$) | Estimated MAN (µmol $g^{-1}$) |
|---|---|---|---|
| E-F-P | 6.6 | 7.1 | 7.1 |
| E-4S-F-P | 7.5 | 8.1 | 8.1 |
| ENE-F-P | 7.0 | 7.6 | 7.6 |
| ENE-4S-F-P | 5.6 | 6.0 | 6.0 |

**Figure S5.** Primary amine assays for AUTES titration using fluorescamine reagent. (a) Formation of fluorescent pyrrolinone by reaction between non-fluorescent fluorescamine (FA) and 11-(aminoundecyl)triethoxysilane (AUTES). (b) Schematic depiction of F-P PMO@PEG NPs functionalized with a 25:1 PEG-Si:AUTES molar ratio. (c) Fluorescence emission spectra of n = 4 standards (FA:AUTES mixtures, converted into pyrrolinone) and associated calibration curve. (d) Measured AUTES grafting amounts in F-P PMO@PEG NPs and associated estimated grafting amounts of AUTES and MAN (*vs.* pristine NPs).

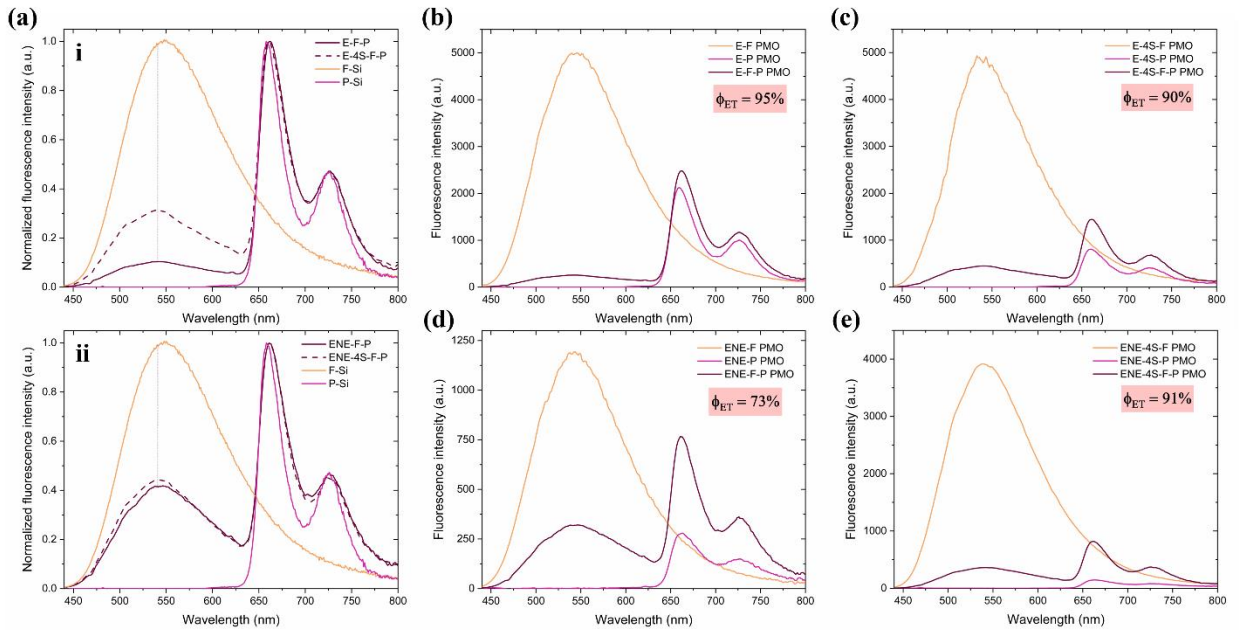


**Figure S6.** Fluorescence emission spectra of chromophore-based PMO NPs and associated one-photon FRET efficiencies. (a) Fluorescence profiles of E-based (i) and ENE-based (ii) F-P PMO NPs *vs.* silylated chromophore precursors. Energy donor-based (F PMO), energy acceptor-based (P PMO) and associated donor-acceptor-based (F-P PMO) NPs emission profiles were compared upon OPE at 413 nm. (b) E PMO NPs emission profiles. (c) E-4S PMO NPs emission profiles. (d) ENE PMO NPs emission profiles. (e) ENE-4S PMO NPs emission profiles. F fluorescence is quenched by P *via* energy transfer, and P emission is increased.

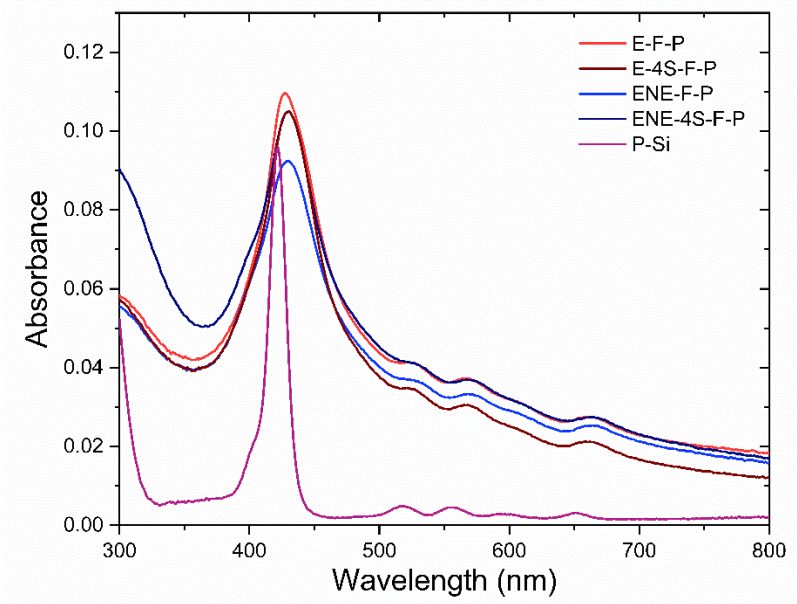


**Figure S7.** Absorbance spectra of F-P PMO NPs and P-Si precursor. A small bathochromic shift and a band broadening are observed due to the formation of J aggregates in NPs. NPs were suspended in EtOH.

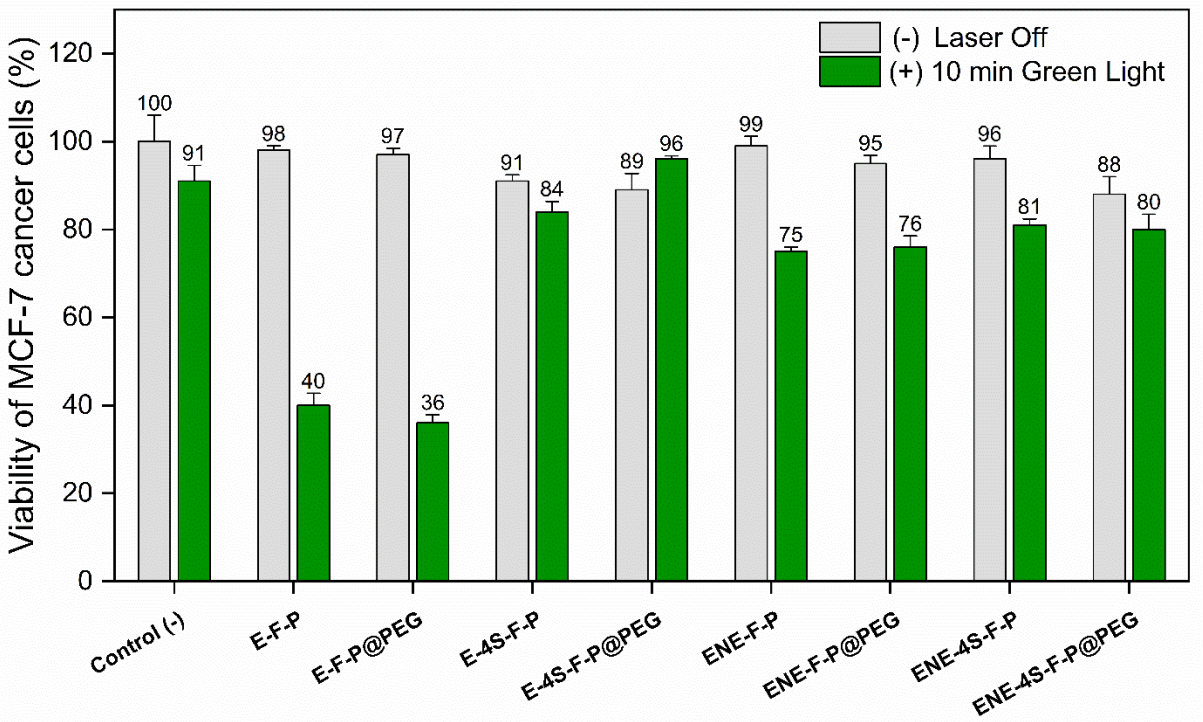


**Figure S8.** One-photon excitation (OPE)-PDT with pristine and PEG-grafted F-P PMO NPs. OPE-triggered MCF-7 cancer cells killing after incubation with NPs at 50 μg $mL^{-1}$ for 24 h and irradiation at 525 nm for 10 min (34 J $cm^{-2}$). Lines represent standard deviations of three independent experiments.

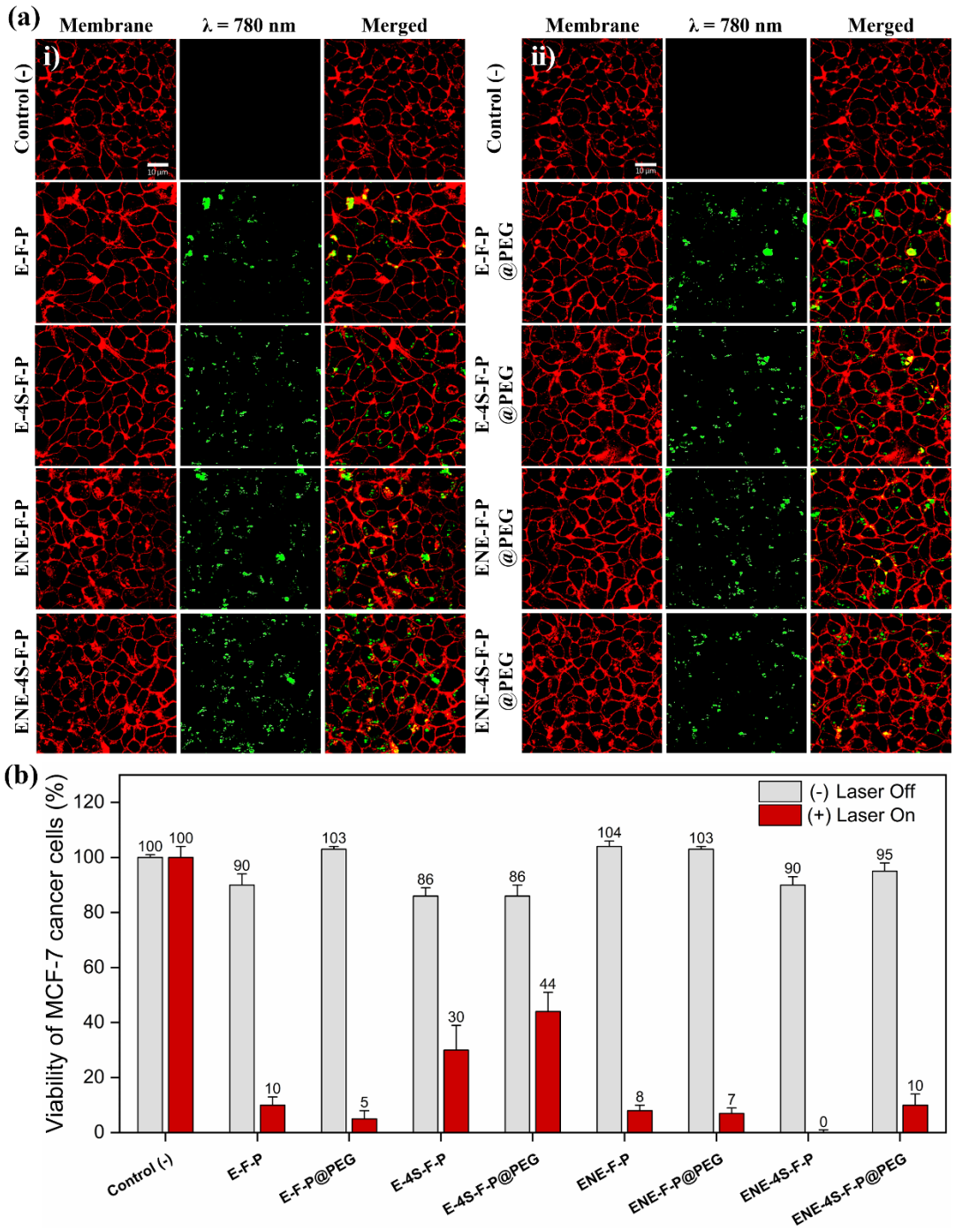


**Figure S9.** Cell internalization and anticancer TPE-PDT assays. (a) Cell internalization study of pristine (i) and PEG-grafted (ii) F-P PMO NPs at 50 µg $mL^{-1}$ using confocal microscopy imaging. After incubation for 24 h, MCF-7 cancer cells were stained with Cell Mask™ Orange Plasma Membrane and then visualized at 561 nm (membrane) and 780 nm (F-P PMO NPs). Images were obtained with Carl Zeiss LSM780 confocal fluorescence microscope using a high magnification (63×/1.4 OIL Plan-Apo). (B) TPE-triggered MCF-7 cancer cells killing after incubation with NPs at 50 µg $mL^{-1}$ for 24 h and irradiation at 780 nm (3 × 1.26 s). Lines represent standard deviations of six or eight independent experiments.

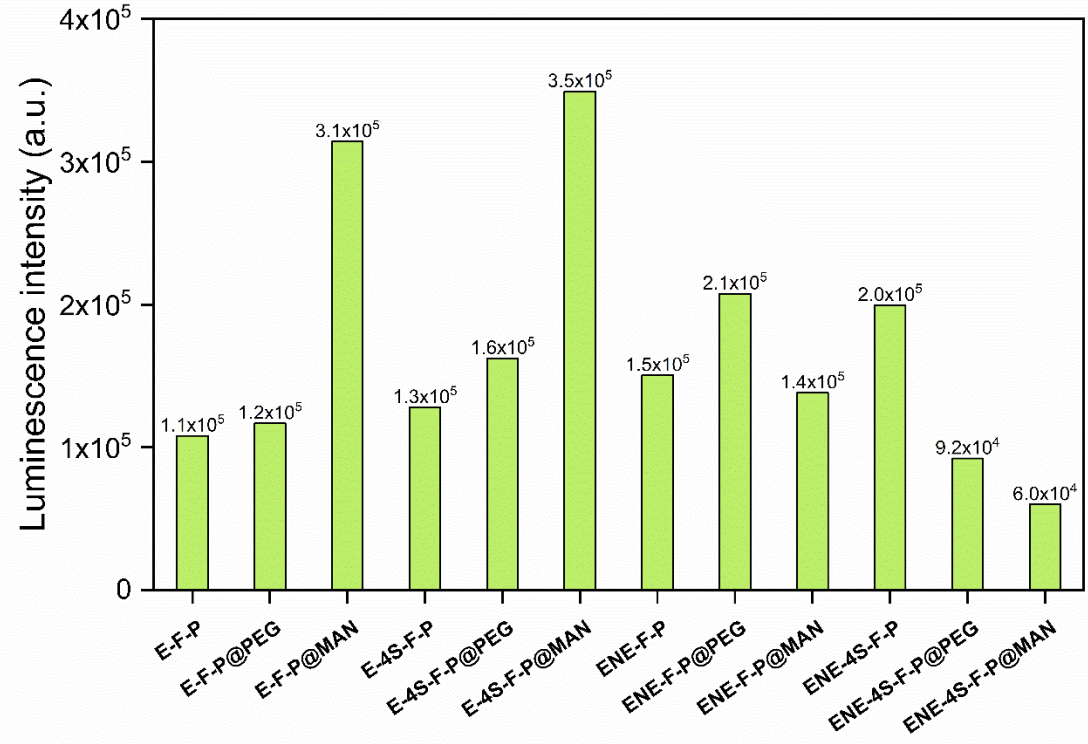


**Figure S10.** Assessment of pristine and multifunctional F-P PMO NPs uptake inside MCF-7 cells after 24 h incubation. All the surface of the pictures obtained by confocal microscopy were submitted to a semi-quantitative evaluation using ImageJ software. Values are levels of NPs luminescence presented in arbitrary units.

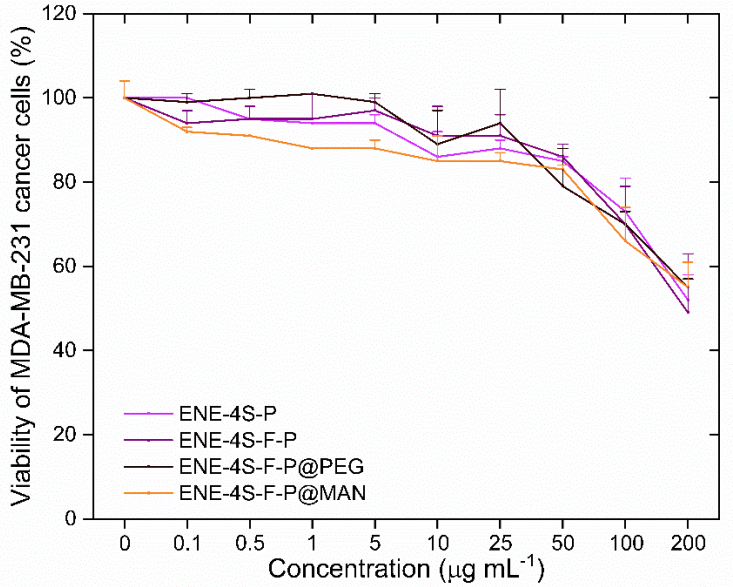


**Figure S11.** Toxicity studies of pristine ENE-4S(-F)-P and functionalized ENE-4S-F-P PMO NPs on human breast MDA-MB-231 cancer cells. Cells were incubated with different concentrations for 72 h. Cell viability data are presented as mean ± standard error of mean of two independent experiments.

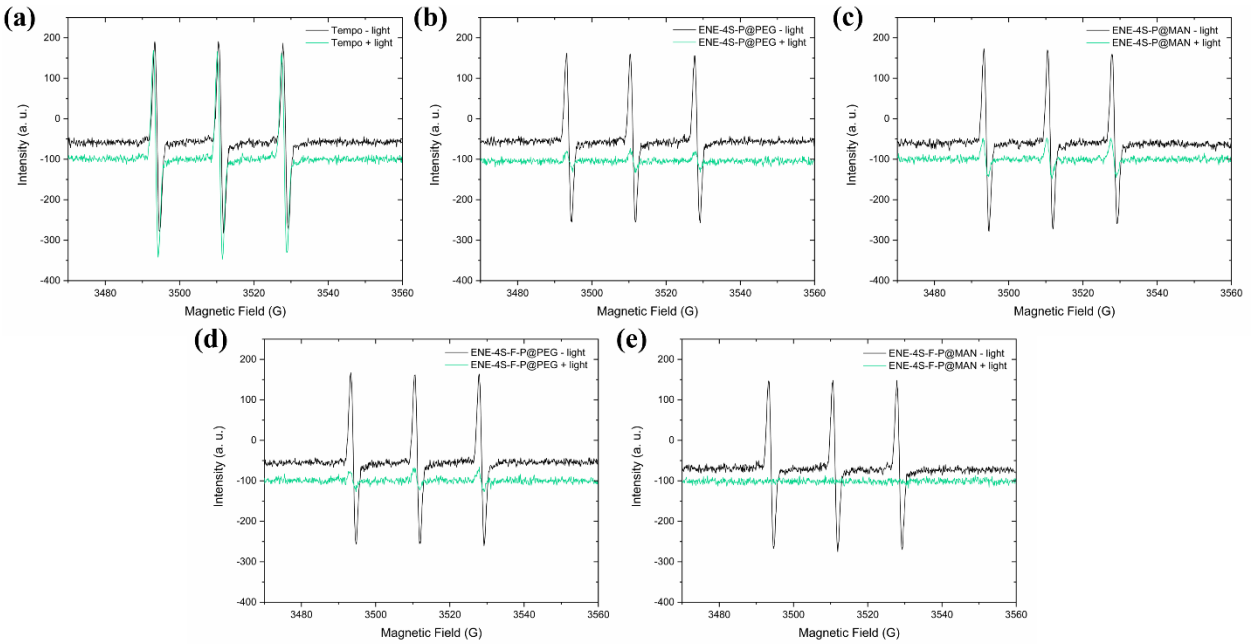


**Figure S12**. ROS generation assay using electron spin resonance (ESR). ESR spectra before and after 15 min of OPE at 450-480 nm with 10 µM TEMPO free radical scavenger and 50 µg $mL^{-1}$ of PMO NPs. (a) Negative control. (b) ENE-4S-P@PEG. (c) ENE-4S-P@MAN. (d) ENE-4S-F-P@PEG. (e) ENE-4S-F-P@MAN.

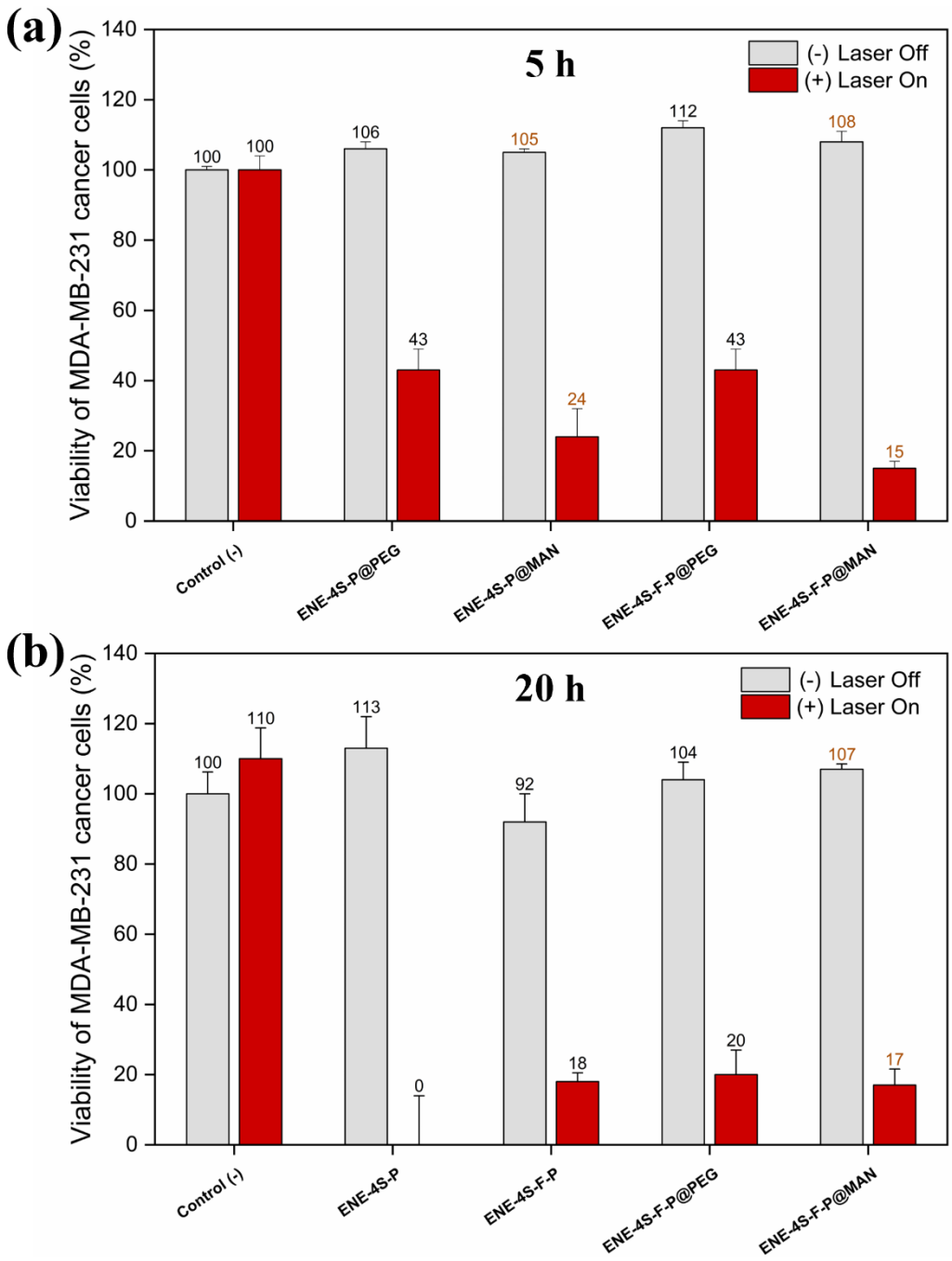


**Figure S13.** Impact of nanoparticles' incubation time and mannose phenyl squarate targeting on TPE-PDT efficiency. TPE-triggered MDA-MB-231 cancer cells killing after incubation with NPs at 50 μg $mL^{-1}$ for (a) 5 h or (b) 20 h, and irradiation at 780 nm (3 × 1.26 s). Lines represent standard deviations of three independent experiments.

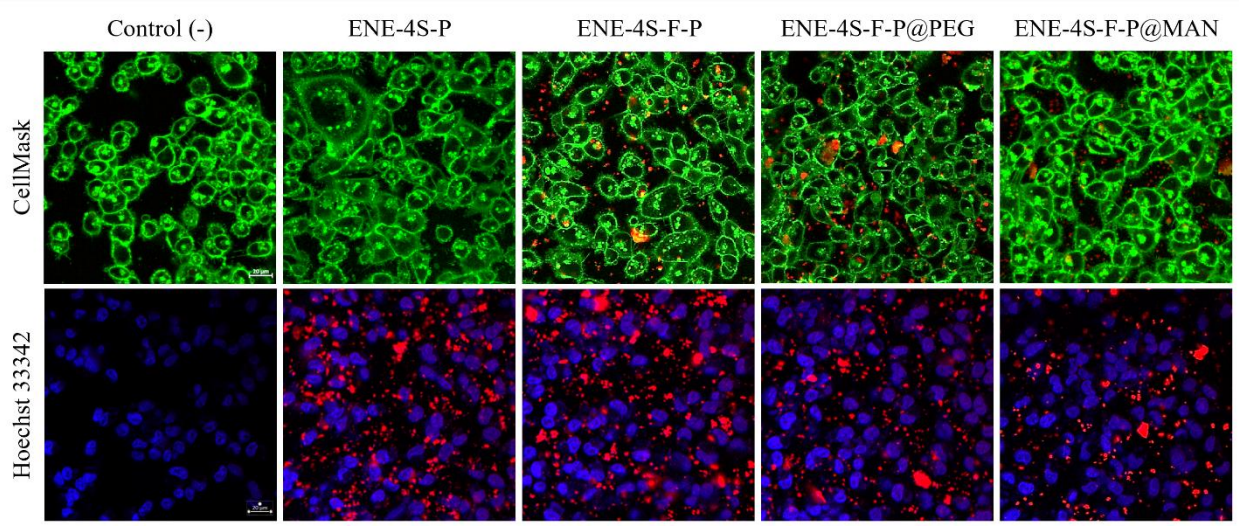


**Figure S14.** Cell internalization of various ENE-4S(-F)-P PMO NPs using the intrinsic emission of chromophores. Cell internalization study of ENE-4S based PMO NPs at 50 µg $mL^{-1}$ using confocal microscopy imaging. After incubation for 24 h, MDA-MB-231 cancer cells were stained with Cell Mask™ Orange Plasma Membrane and with Hoechst 33342™ then visualized at 561 nm (membrane), 405 nm (nuclei) and 780 nm (F-P PMO NPs). Images were obtained with Carl Zeiss LSM780 confocal fluorescence microscope using a high magnification (63×/1.4 OIL Plan-Apo). The characteristics of these nanoparticles (F emission: 500-550 nm; P emission: 632-694 nm;) allow to choose the fluorescence emission range to collect their signal, to avoid overlap with Cell Mask and Hoechst stains.

# REFERENCES


1 S. Brunauer, P. H. Emmett and E. Teller, *J. Am.Chem.Soc.*, 1938, **60**, 309–319.

2 M. I. López, D. Esquivel, C. Jiménez-Sanchidrián, P. Van Der Voort and F. J. Romero-Salguero, *J. Phys. Chem. C*, 2014, **118**, 17862–17869.

3 J. Croissant, X. Cattoën, M. Wong Chi Man, A. Gallud, L. Raehm, P. Trens, M. Maynadier and J. O. Durand, *Adv. Mater.*, 2014, **26**, 6174–6180.

4 B. Mezghrani, L. M. A. Ali, S. Richeter, J. O. Durand, P. Hesemann and N. Bettache, *ACS Appl. Mater. Interfaces*, 2021, **13**, 29325–29339.